Crossing-Lines Registration for Direct Electromagnetic Navigation

Brian J. Rasquinha, Andrew W.L. Dickinson, Gabriel Venne, David R. Pichora, and Randy E. Ellis

Queen's University, Kingston, Canada

Abstract. Direct surgical navigation requires registration of an intraoperative imaging modality to a tracking technology, from which a patient image registration can be found. Although electromagnetic tracking is ergonomically attractive, it is used less often than optical tracking because its lower position accuracy offsets its higher orientation accuracy.

We propose a crossing-lines registration method for intraoperative electromagnetic tracking that uses a small disposable device temporarily attached to the patient. The method exploits the orientation accuracy of electromagnetic tracking by calculating directly on probed lines, avoiding the problem of acquiring accurately known probed points for registration. The calibration data can be acquired and computed in less than a minute (50 s $\pm$ 12 s). Laboratory tests demonstrated fiducial localization error with sub-degree and sub-millimeter means for 5 observers. A pre-clinical trial, on 10 shoulder models, achieved target registration error of 1.9 degree $\pm$ 1.8 degree for line directions and 0.8 mm $\pm$ 0.6 mm for inter-line distance. A Board-certified orthopedic surgeon verified that this accuracy easily exceeded the technical needs in shoulder replacement surgery.

This preclinical study demonstrated high application accuracy. The fast registration process and effective intraoperative method is promising for clinical orthopedic interventions where the target anatomy is small bone or has poor surgical exposure, as an adjunct to intraoperative imaging.

1 Introduction

Direct surgical navigation is a subset of image-guided surgery where the guidance image is acquired intraoperatively, using modalities such as MRI, 3D fluoroscopy or ultrasound [9,12,4]. A limiting constraint on direct navigation is the registration of the image to the 3D tracking system, for which simultaneous tracking of the imaging device and the patient has proven so cumbersome as to prevent widespread adoption. Although preoperative calibration is an effective option for floor-mounted imaging [11], mobile-imaging devices remain a challenge.

The most used tracking technology for direct navigation is optical localization. Major drawbacks are maintaining a line of sight – the principal reason that direct navigation is not more prevalent – and, for small or deep anatomy such as the bones of the shoulder, the optical devices are too large to be rigidly affixed to thin fragile bone. Another prevalent tracking technology uses electromagnetic

N. Navab et al. (Eds.): MICCAI 2015, Part II, LNCS 9350, pp. 321–328, 2015.
DOI: 10.1007/978-3-319-24571-3_39

(EM) physics. EM is superior to optical technology by being very lightweight – a sensor is an antenna with electrical leads, often sub-millimeter in diameter – and avoiding line-of-sight problems. The major drawback is that, even when used far from conductive materials, EM has less positional accuracy than optical tracking [6,8], in some cases with errors increasing by an order of magnitude between laboratory and clinical settings [7]. Intriguingly, EM appears to have high inherent orientation accuracy for common two-coil 6DOF trackers [10] that might be useful for a novel kind of image-tracking registration.

The method is a fast, accurate intraoperative registration method for EM-tracking that needs no preoperative calibration or anatomical probing. The mathematics are an adaptation of X-ray source localization by computation of lines that cross in space. The concept is to affix a small, lightweight plastic device to the target anatomy, then probe linear paths to achieve a registration. An example application is reverse shoulder replacement surgery, where the tip of a drill is visible to the surgeon and the drill orientation is critically important but difficult to achieve without image-based navigation. The technique was tested on 10 models of cadaveric shoulders and produced sub-millimeter accuracy.

2 Materials and Methods

Two kinds of methods were used: computational and empirical. Materials were manufactured by the authors; some were derived from CT scans of cadaveric donations, the latter approved by the relevant Institutional Review Board.

The fundamental datum was a line, which was a point $\vec{p}$ and a signed direction vector $\vec{d}$ (i.e., a spatial point on the unit sphere). A previous registration method [5] uses line data to establish correspondences, but not as registration features. The fundamental sources were EM tracking of a pointed cylindrical surgical probe and the planned directions of linear holes in a calibration device.

2.1 Computational Methods

Our registration problem was estimation of a rigid transformation from the electromagnetic coordinate frame $\boldsymbol{E}$ to the calibrator coordinate frame $\boldsymbol{C}$. As is usual, we separated this into orientation estimation and translation estimation. Each estimate was found using a somewhat novel variant of previous methods.

For orientation, we paired a tracked probe direction ${}^{E}\vec{d}$ with a planned calibrator hole direction ${}^{C}\vec{d}$. Rather than thinking of these as direction vectors, we interpreted them as points on the unit sphere; n of these spherical points could be registered using Arun's method [3]. A least-squares registration transformation ${}^{C}_{E}R$ from frame $\boldsymbol{E}$ to frame $\boldsymbol{C}$, which minimizes the residual distances between the sets of points, can be computed from Sibson's 3×3 data matrix H [13] using the singular-value decomposition (SVD) as

$$
\begin{aligned}
H = \sum_{i=1}^{n} \left({}^{C}\vec{d}_i \, {}^{E}\vec{d}_i^{\,T} \right) &= U \Sigma V^T \\
\Rightarrow \quad {}^{C}_{E}R &= V U^T
\end{aligned}
\tag{1}
$$

Cases with $\det(VU^T) \neq 1$ were rejected as geometric singularities [3]. This solved the orientation problem without using points, needing only directions $\vec{d}_i$.

To estimate the translation component, a variant of "crossing-lines" was used. Crossing-lines has been used extensively in 2D virtual fluoroscopy to determine the X-ray source location from an image that contains tiny fiducial markers; this is illustrated in Figure 1(a) and a corresponding calibration device, with holes that guide 7 lines, is shown in Figure 1(b). The mathematics are straightforward: let $\vec{c}$ be the nominal crossing point of n lines in space. Minimization of the distance between $\vec{c}$ and the i^{th} line $\vec{l}(\lambda) = \vec{p}_i + \lambda\vec{d}_i$, over all n lines, can be found in the least-squares sense by solving the overdetermined linear equation

$$\left(\sum_{i=1}^{n}\left(I - \vec{d}_i\vec{d}_i^T\right)\right)\vec{c} = \sum_{i=1}^{n}\left(\left(I - \vec{d}_i\vec{d}_i^T\right)\vec{p}_i\right) \tag{2}$$

The value $\vec{c}$ in Equation 2 was computed from the QR decomposition. Together, ${}^C_ER$ and $\vec{c}$ constituted a least-squares registration solution that depended primarily on the direction vectors $\vec{d}_i$ and to a lesser degree on the point positions $\vec{p}_i$; this took great advantage of the orientation accuracy of EM sensing.

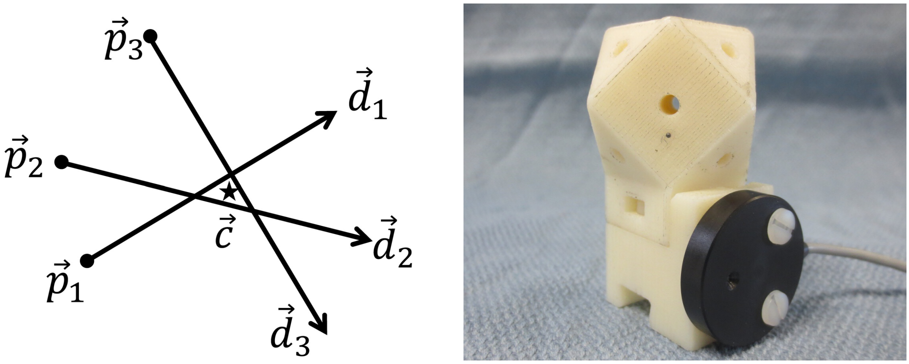

Fig. 1. Crossing-lines for registration. (left) From lines that contain points $\vec{p}_i$ and have corresponding directions $\vec{d}_i$, the center of crossing $\vec{c}$ can be estimated in a least-squares sense. (right) A device was additively manufactured to constrain 7 such lines.

2.2 Calibration Device

A cuboctahedral calibration device was additively manufactured in ABS plastic, shown in Figure 1(b). Seven tantalum beads, for CT verification in subsequent work, were fixed in dimples in the device faces: three in the top face and one in each vertical face. The device included 7 through holes that physically provided 7 crossing lines. The design files were used to establish the calibrator coordinate frame $\boldsymbol{C}$, with each hole axis giving a direction vector ${}^C\vec{d}_i$.

An Aurora 6-DOF disc EM sensor (NDI, Waterloo, CA) was fixed to the device using two nylon 4-40 machine screws. The disc was used to establish the EM coordinate frame $\boldsymbol{E}$, in which pointer directions ${}^{E}\vec{d}_i$ were measured.

2.3 Tracking Hardware and Software

During EM tracking, a manufacturer's standard surgical probe was used to gather position data from its tip and direction data from its axis. Custom C++ software gathered data at ≈ 45 Hz, averaging 45 consecutive readings as unsigned axial means [1]. Translations were averaged linearly. All tests representing intra-operative activities (Sections 2.5 and 2.6) were conducted in a surgical operating room, thus reproducing representative sources of EM interference. Cone beam computed tomography (CBCT) scans in these sections were performed using an Innova 4100 (General Electric, Waukesha, US) at a 0.46 mm voxel size.

2.4 Fiducial Localization Error (FLE)

Because registration was computed from paired lines, the Fiducial Localization Error (FLE) was also calculated from the lines. The paired lines were, respectively, sensed by the EM tracker and derived from the calibrator design file. Each angular FLE was the angular difference between each matched pair of skew lines. The distance FLE was the minimal normal distance between the infinitely long skew lines, which was the formulation used in the registration algorithm.

Using a consistent experimental setup in a laboratory environment, five subjects (the co-authors) collected data for FLE assessment. For one trial, each subject probed each hole of the calibrator for approximately 1 s; this produced 7 lines per subject. Each subject performed 5 trials, totalling 35 lines per subject.

The line FLEs of each subject were pooled to find mean and standard deviations. Subject performance was assessed by comparing the pooled line FLEs to the best accuracies found in the literature, which were $1°$ in direction and 0.5 mm in translation. The line FLEs of all subjects were further pooled.

Based on the line FLE findings, we conducted a detailed accuracy assessment using data collected by one investigator (DRP, an orthopedic surgeon).

2.5 Point Target Registration Error (Point TRE)

Point-to-point positioning was assessed using a custom accuracy apparatus, which was an additively manufactured ABS plate that incorporated a dovetail for mounting the calibrator. Fourteen 0.8 mm tantalum beads were fixed in a planar spiral, at $60°$ with 5 mm spacing; the apparatus is pictured in Figure 2.

Point target registration error (point-TRE) was assessed in an operating room with the calibrator fixed to the apparatus. Each bead was probed for ≈ 1 s with the 6DOF probe by one subject (author DRP). The position and direction of the probe were recorded relative to the calibrator-fixed EM sensor. After EM collection, CBCT images of the point-TRE apparatus were acquired and the beads were manually segmented.

EM measurements were transformed to the CBCT frame using the calibrator transform and the residuals between paired features were used as the point-TRE measurement. This represented an end-to-end system accuracy, incorporating the errors in segmentation, calibration, and tracking of a surgical work-flow.

2.6 Line Target Registration Error (Line-TRE)

Line target registration error (line-TRE) was assessed using preparations from shoulder arthroplasty. Ten cadaveric shoulders, with no specimen having a history of surgical intervention, were scanned using axial CT at 0.49 mm resolution and 0.63 mm slice spacing. Each scapula scan was manually segmented and a Board-certified surgeon planned paths for a reverse shoulder arthroplasty base-plate peg and four implanting screws; this produced five target lines in each cadaver image volume. Each line was modeled as a 3 mm diameter cylinder that was subtracted from the segmented scapula. Previous studies using this workflow and equipment replicated bony geometry to submillimeter accuracy as compared to laser scans of dry bones [2].

A male dovetail was added to the coracoid process of each scapula for calibrator fixation. Each modified scapula was additively manufactured in ABS plastic. An example line-TRE scapula is pictured in Figure 2.

For each scapula, two titanium screws were placed in the dovetail to allow for EM tracking alterations that might occur during clinical fixation. The calibrator was affixed and each drill path was probed by the planning surgeon using the 6DOF EM probe. As in Section 2.5, ≈ 1 s of relative pose measurements were collected in an operating room and the probe position and direction relative to the calibrator were averaged. The scapula and affixed calibrator were then scanned with CBCT and manually segmented. Each original 3D design file was registered to the segmented CBCT models using an ICP algorithm. This registration transformed the planned screw and base-plate peg lines to the CBCT coordinate frame. The transformed planned lines were compared to the EM probed lines.

The line-TRE was assessed using the line-FLE methods, which were the angles between paired direction vectors and the minimum paired line-line distance. These measurements represented an end-to-end error assessment that closely simulated the error expected in surgical navigation.

3 Results

Paired line calibrations were performed with an average time of 50 s $\pm$ 12 s, including data collection and calculating the calibrator transform; each of 5 observers acquired 7 consecutive lines, 5 times each. Fiducial localization errors (FLEs) from these calibrations are presented in Table 1. The FLEs were consistently below manufacturer reported errors, which were 1° in orientation accuracy and 0.5 mm in position accuracy. Based on these excellent results, a single observer was chosen for the TRE experiments.

A single observer, highly experienced in data acquisition and use of computer-assisted surgery, touched each of the 14 beads in the point-TRE apparatus with

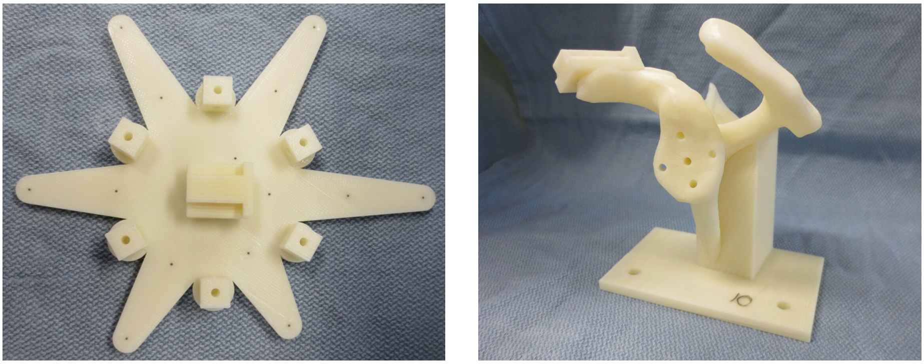

Fig. 2. Point TRE device (left) and Line TRE device (right); no calibrator present.

Table 1. Summary of Fiducial Localization Error (FLE) for each investigator and with all investigators pooled. None of these error groups were found to be statistically significantly higher than 1° or 0.5 mm using a one-sided, one sample t-test ($\alpha = 0.95$).

	Observers, by alphabetic code; 35 lines per observer					
	A	B	C	D	E	Pooled
Angular FLE (°)	0.7 ± 0.3	0.8 ± 0.3	0.4 ± 0.2	0.8 ± 0.4	0.8 ± 0.4	0.7 ± 0.4
Distance FLE (mm)	0.3 ± 0.2	0.3 ± 0.3	0.3 ± 0.2	0.3 ± 0.2	0.4 ± 0.3	0.3 ± 0.2

the pointed EM-tracked probe. After transforming the EM readings into a CT-derived coordinate frame, the residual point-TRE experiment had an accuracy of 2.3 mm $\pm$ 0.8 mm.

The same single observer later acquired 5 lines for each line-TRE scapula, the lines being preoperatively planned drill holes that were manufactured into each scapula. Detailed line-TRE results are presented in Table 2. In summary, the line-TRE, pooling all 5 lines of 10 scapular models, had an overall angular error

Table 2. Summary of Line Target Registration Errors (Line-TRE). For each line-TRE scapula, line-line angles were assessed using the skew angle between the lines; means (μ) and standard deviations (σ) are reported for the 5 lines used for each scapula. Likewise, line-line distances were assessed using the minimum normal distance between the 5 lines for each scapula. Pooled results are for all 50 lines.

	Line-TRE scapula, by code; 5 lines per scapula										
	S01	S02	S03	S04	S05	S06	S07	S08	S09	S10	Pooled
Angular TRE μ (°)	2.4	1.1	1.6	0.8	2.8	3.3	2.4	2.0	0.9	1.3	1.9
Angular TRE σ (°)	1.6	1.3	0.6	0.8	4.0	2.7	1.4	0.3	1.3	0.3	1.8
Distance TRE μ (mm)	1.2	1.5	0.4	0.8	0.5	1.2	1.1	1.2	1.3	1.4	1.1
Distance TRE σ (mm)	0.7	0.4	0.3	0.5	0.3	1.0	0.5	0.9	1.0	0.9	0.7

of 1.9°± 1.8° of skew angle between the actual EM probe line and the physical hole in CT-derived coordinates. The line-line distance was 1.1 mm ± 0.7 mm, assessed as being the minimum normal distance between the two lines.

4 Discussion

Electromagnetic tracking for surgical navigation is ergonomically preferred over optical tracking in procedures where sensor size and line-of-sight are major concerns. One impediment of EM has been its relatively poor point-localization accuracy, which precludes the use of surface-based registration algorithms on small anatomical targets. Poor localization leads to poor registration, which may have limited the adoption of EM technology in high-accuracy surgical applications.

This work largely avoids the potentially poor point localization of EM by instead relying on its superior orientation accuracy. Decoupling a rigid registration into an orientation problem and a translation problem, the orientation problem was solved by interpreting directions as points on a sphere and adapting previous point-based methods to estimate a least-squares orientation. The translation problem was solved by modifying a method from X-ray calibration to register multiple lines that cross in space, combining direction and position measurements so that positions were relied on as little as possible.

The point-based FLE was consistently below 0.5 mm and 1°, which suggests an excellent match between the sensed axis of a tracked EM probe and its CT-based location. Conventional measurement of TRE was 2.3 mm ± 0.8 mm, which is consistent with the literature [6,10].

The line-TRE, pooling 50 acquisitions by a single observer, was 1.9° ± 1.8° in angle and 1.1 mm ± 0.7 mm in distance. The angular accuracy is close to what is found in surgical navigation based on optical tracking, where orientation must be inferred from a rigid array of markers. The distance accuracy is also close to optical tracking, with the caution that this measures line-line distances whereas most navigation work reports point-point distances.

This work suggests that EM tracking can provide excellent accuracy from intraoperative data collection and calibration that requires less than a minute to perform. Future developments of this system towards clinical practice include automating the current manual segmentation step of the workflow and verifying the results on these phantoms with drilling tasks on cadaveric specimens.

Although EM navigation has fundamental physics limitations, such as field alteration by external objects, this work is an example of how relatively low positioning accuracy can be overcome by using the relatively high orientation accuracy of EM tracking in a disciplined registration framework. A crossing-lines registration apparatus can be temporarily added to an electromagnetic surgical tracking device that is already affixed to a patient, solving an existing problem in direct surgical navigation with a simple combination of hardware and software. Further, this registration technique can be applied to any tracking modality with a calibrated probe, including optical tracking.

The prominent surgical opportunity is for direct navigation of small orthopedic targets, for which optical devices are too large or heavy to be practical.

An example is the shoulder glenoid, where perforation of the thin scapula when drilling presents considerable risk of post-surgical complications. Such an application exploits the main accuracy of EM – direction determination – and supplements a surgeon's conventional positioning accuracy within a clear surgical exposure. Future work may include clinical trials of the device, particularly in the shoulder and wrist, for treatment of early-onset arthritis or to repair poorly healed fractures in or around a joint.

References

1. Amaral, G.J.A., Dryden, I.L., Wood, A.T.A.: Pivotal bootstrap methods for k-sample problems in directional statistics and shape analysis. J. Am. Stat. Assoc. 102(478), 695–707 (2007)
2. Anstey, J.B., Smith, E.J., Rasquinha, B., Rudan, J.F., Ellis, R.E.: On the use of laser scans to validate reverse engineering of bony anatomy. Stud. Health Technol. Inform., 18–24 (2011)
3. Arun, K.S., Huang, T.S., Blostein, S.D.: Least-squares fitting of two 3-D point sets. IEEE Trans. Pattern Anal. Mach. Intell. 9(5), 698–700 (1987)
4. Chopra, S.S., Hünerbein, M., Eulenstein, S., Lange, T., Schlag, P.M., Beller, S.: Development and validation of a three dimensional ultrasound based navigation system for tumor resection. Eur. J. Surg. Oncol. 34(4), 456–461 (2008)
5. Deguchi, D., Feuerstein, M., Kitasaka, T., Suenaga, Y., Ide, I., Murase, H., Imaizumi, K., Hasegawa, Y., Mori, K.: Real-time marker-free patient registration for electromagnetic navigated bronchoscopy: a phantom study. Int. J. Comput. Assist. Radiol. Surg. 7(3), 359–369 (2012)
6. Frantz, D.D., Wiles, A.D., Leis, S.E., Kirsch, S.R.: Accuracy assessment protocols for electromagnetic tracking systems. J. Phys. Med. Biol. 48(14), 2241–2251 (2003)
7. Franz, A.M., Haidegger, T., Birkfellner, W., Cleary, K., Peters, T.M., Maier-Hein, L.: Electromagnetic tracking in medicine-a review of technology, validation and applications. IEEE. Trans. Med. Imag. 33(8), 1702–1725 (2014)
8. Hummel, J.B., Bax, M.R., Figl, M.L., Kang, Y., Maurer Jr., C., Birkfellner, W., Bergmann, H., Shahidi, R.: Design and application of an assessment protocol for electromagnetic tracking systems. J. Med. Phys. 32(7), 2371–2379 (2005)
9. Jolesz, F.A., Navabi, A., Kikinis, R.: Integration of interventional MRI with computer- assisted surgery. J. Magn. Reson. Imaging 13(1), 69–77 (2001)
10. Lugez, E., Sadjadi, H., Pichora, D.R., Ellis, R.E., Akl, S.G., Fichtinger, G.: Electromagnetic tracking in surgical andinterventional environments: usability study. Int. J. Comput. Assist. Radiol. Surg. 10(3), 253–262 (2014)
11. Oentoro, A., Ellis, R.E.: High-accuracy registration of intraoperative CT imaging. In: SPIE Med. Imaging, pp. 762505–762505 (2010)
12. Smith, E.J., Al-Sanawi, H., Gammon, B., Ellis, R.E., Pichora, D.R.: Volume rendering of 3D fluoroscopic images forpercutaneous scaphoid fixation: An in vitro study. Proc. Inst. Mech. Eng. H 227(4), 384–392 (2013)
13. Sibson, R.: Studies in the robustness of multidimensional scaling: Procrustes statistics. J. Royal. Stat. Soc. B 40(2), 234–238 (1978)